Magnetization properties and irreversibility lines of $YBa_2Cu_3O_y/PrBa_2Cu_3O_y$ multilayered films

H. Obara, A. Sawa, and S. Kosaka
Electrotechnical Laboratory, 1-1-4 Umezono, Tsukuba, Ibaraki 305, Japan
(Received 25 August 1993)

Systematic measurements were made of the dc magnetization in multilayered $YBa_2Cu_3O_y$/$PrBa_2Cu_3O_y$ (YBCO/PBCO) films. The films were fabricated using a molecular-beam-epitaxy technique and were oriented with their c axis perpendicular to the substrate. A magnetic field was applied that was both perpendicular to the films and parallel to the film's c axis. The irreversibility lines of the films were determined to be at the temperature and the magnetic field when the remanent magnetization falls below the detection limits of the instrumentation. We observed that the irreversibility line of a film strongly depends on the thickness of the YBCO layers. On the other hand, for the same thickness of YBCO layer, the irreversibility lines did not change (except for a slight change in the superconducting transition temperature T_c) for YBCO/PBCO multilayered films having PBCO layers that were from three to eight unit cells thick. The YBCO layers appeared to completely decouple when the PBCO layer was thicker than three unit cells. As observed in other high-T_c materials, the temperature dependence of the irreversibility field for these films exhibited a power-law behavior predicted by a thermally activated flux-flow (TAFF) model near T_c, and deviated from this behavior at temperatures below $T/T_c \sim 0.6$, where T is temperature. Irreversibility lines of YBCO/PBCO multilayered films are considered to be analogous to those of Bi systems, which are more anisotropic than YBCO systems. Relaxation of the magnetization for the films were also measured and the electric field vs current density (E-J) characteristics were estimated. These estimates suggest the existence of vortex glass state at relatively low temperature. In the temperature dependence of the remanent magnetization in the films that had very thin YBCO layers, another transition was observed below the irreversibility line. The E-J characteristics, scaled using this transition temperature, suggest that this transition is the vortex glass transition and that there are two kinds of vortex states below the irreversibility line, i.e., vortex liquid and vortex glass. From these experimental results, the vortex states and anisotropy of high-T_c superconductors were then discussed from the standpoint of both the TAFF model and the vortex glass model.

I. INTRODUCTION

$YBa_2Cu_3O_y/PrBa_2Cu_3O_y$ (YBCO/PBCO) multilayered films have been extensively studied, because PBCO has the same crystal structure as YBCO, although the resistivity of PBCO exhibits a semiconductive temperature dependence. Good-quality YBCO/PBCO multilayered films have been prepared using techniques such as sputtering,[1,2] laser deposition,[3,4] and coevaporation (e.g., molecular beam epitaxy, MBE).[5,6] One purpose of such studies was to apply high-T_c superconductors to electronic devices. Another purpose was to observe intrinsic properties of very thin films of oxide superconductors, because the fabrication technique of very thin YBCO layers sandwiched between PBCO layers has now been established and anisotropy of such a system can be controlled artificially. The dynamics of flux in YBCO/PBCO multilayers have been recently discussed in terms of the properties of thin films. Brunner *et al.*[7] carefully measured the resistive transition of YBCO/PBCO multilayers, and observed that the thermally activated flux flow (TAFF) was enhanced as the thickness of the YBCO layers was decreased. Moreover, Matsuda *et al.*[8] reported a Kosterlitz-Thouless (KT) transition in a very thin (one cell thick) YBCO film sandwiched between PBCO layers. These results indicate that flux motion in high-T_c materials is strongly correlated with the large anisotropy and the two dimensionality of superconductors.

Recently, special attention has been given to the vortex glass model. As Dekker *et al.* observed in very thin YBCO films,[9] the vortex glass transition depends on the dimensionality of superconductors. In order to discuss the vortex state of high-T_c superconductors, many measurements of irreversibility lines have been made.[10] From the standpoint of the vortex glass model, a irreversibility line is considered to be related to the melting transition of vortex glass and to be correlated with the strong anisotropy of high-T_c superconductors. The irreversibility field of YBCO is much higher than that of Bi systems that are more anisotropic. Using the YBCO/PBCO multilayered films, we can control the anisotropy of superconductors by changing the thickness of the YBCO and PBCO layers, consequently making YBCO/PBCO multilayers suitable for a model system of high-T_c superconductors.

The main purpose of our study here is to observe the magnetization properties of YBCO/PBCO multilayered films. Transport properties of such films have been extensively studied. However, not only do conventional transport measurements depend on the current path, but also

0163-1829/94/49(2)/1224(9)/$06.00

the effects of inhomogeneity are not negligible. On the other hand, magnetization measurements are powerful in evaluating the flux dynamics of the entire film sample.

In the present work, we measured the dc magnetization of YBCO/PBCO multilayers using a superconducting quantum interference device (SQUID) magnetometer, and determined the irreversibility line of the films to be at the temperature and the magnetic field at the point when the remanent magnetization fell below the detection limits of our instruments. We also measured the relaxation of the magnetization to observe electric field vs current density (E-J) characteristics for the films. Finally, we discussed the vortex state of YBCO/PBCO multilayers from the standpoints of the TAFF and of the vortex glass model to understand the correlation between anisotropy and the vortex states of high-T_c superconductors.

II. EXPERIMENTAL DETAILS

A. Thin film preparation

Thin films were prepared using an MBE technique with pure ozone. The evaporation sources were four effusion cells (maximum temperature of 1800 °C), where the Y, Ba, Cu, and Pr metal elements were individually evaporated. Ba and Cu were continuously evaporated, and the layered structure of YBCO/PBCO multilayers was controlled by shutters on the Y and the Pr sources. The deposition rate was typically about 0.02 nm/sec. The substrates were a $SrTiO_3$ (100) plane and kept at a temperature of about 650 °C during the deposition, and the films were oriented with their c axis perpendicular to these substrates. For oxidation of the samples, we used pure ozone. The high-purity ozone flux was first evaporated from the liquified ozone and then introduced to the growth chamber during the deposition and the cooling process of the samples. A typical value of the amount of reactive oxygen flux was 10^{14}–10^{15} $cm^{-2}\,sec^{-1}$, almost one order more than that of the metal-element flux. Moreover, we used a differential pumping system, where the evaporation sources were in a vacuum of approximately 10^{-7} Torr and the sample was in a vacuum of approximately 10^{-5} Torr. This system allowed us to not only maintain a stable rate of evaporation for metal elements, but also to obtain effective oxidation of the samples. Using the MBE technique, we successfully fabricated good-quality YBCO films and YBCO/PBCO multilayers. In the present study, very thin, single YBCO layers were sandwiched between PBCO layers to prevent the degradation of the YBCO layers.

B. Magnetization measurements

The magnetization measurements were made using a SQUID magnetometer (Quantum Design MPMS system). Thin film samples were cut parallel to the (010) and (001) plane of the $SrTiO_3$ substrates, and were almost square in shape. The samples were set in a high-purity quartz tube which had very low magnetization, and a magnetic field was then applied perpendicular to the films, i.e., parallel to the c axis of the YBCO films and the YBCO/PBCO multilayers. In a previous study, we carefully measured the sample size dependence of magnetization of thin films using a micropatterning technique.[11] For high field ($\geq$ 1 T) measurements, we used a sample scan length of 2 cm, thus eliminating the effect of inhomogeneous magnetic fields within the SQUID magnetometer.

To determine the irreversibility line, we measured the remanent magnetization of the films. First, a magnetic field was applied to a sample that was well above T_c. The sample was then cooled and the magnetic field was reduced by several hundred Oe (200 Oe was typical for our films), until the sample reached critical state. The remanent magnetization measurements were carried out in a magnetic field higher than 0.1 T, where the distribution of the magnetic field in the thin films was negligible. The critical-current density of the films was calculated using a simple, Bean critical state model. In previous work,[11] we measured the sample size dependence of the remanent magnetization for the YBCO films and confirmed that a Bean critical state is well established in the good-quality epitaxial films prepared using the MBE technique. Finally, the irreversibility line was determined to be at the temperature and the magnetic field at the point when the remanent magnetization goes to zero, i.e., when J_c becomes zero. The resolution of the magnetization measurements was 10^{-7} emu, which corresponds to a J_c of 1000 A/cm^2 for typical thin films. We determined the irreversibility line when the J_c became less than 1000 A/cm^2, which is on the same order as the criterion for transport measurements. The estimated voltage criterion in conventional magnetization measurements, however, is very low ($\sim 10^{-10}$ V/cm) compared with transport measurements.

Relaxation measurements of the magnetization for the films were also performed using the SQUID magnetometer. The E-J characteristics of the films were determined from the time dependence of magnetization, neglecting the geometric factor of the square-shaped samples. Even though time dependence of magnetization cannot be observed on the scale of several minutes using a conventional SQUID magnetometer, precise measurements of small magnetization on the long scale of several hours (which are important in the measurements of thin films) are possible.

III. RESULTS

A. Characterization of films

Flatness of the films is very important in the fabrication of a continuous layered structure that has layers several cells thick. We evaluated this characteristic using two methods: x-ray diffraction (XRD) spectra and the atomic force micrograph (AFM). Figure 1 shows the XRD spectra in the low-angle region of the four-cell-thick

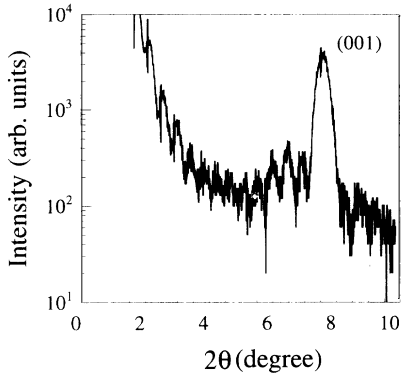

FIG. 1. X-ray diffraction spectra in the low-angle region of a typical YBCO/PBCO multilayered film, where the total thickness of the film was about 20 nm.

YBCO films sandwiched between PBCO layers. The substrate was a $SrTiO_3$ (100) plane, and the c axis of the film was perpendicular to the substrate. Total thickness of the film was 20 nm. Clear finite-size peaks can be seen in the spectra in the figure, and high orders of these finite-size peaks indicate that the thickness fluctuation of the film was very small, confirming that the film was very flat.

Figure 2 shows the AFM image of the same PBCO/YBCO/PBCO layered structure. In general, the surface of the film was flat, except for a few steps that were almost one unit cell (1.2 nm) or two unit cells of YBCO in height.

The results of these evaluations confirm that continuous layered structures with layers more than three unit cells thick can be successfully fabricated using the present MBE technique. In the case of thinner films, namely, less than three unit cells thick, however, island structures appear and the layered structures become discontinuous. When the thickness of YBCO layers was less than three unit cells, we observed a rapid decrease in the magnetization due to the island structures in very thin YBCO layers. Consequently, in the present work, we prepared films that had layers more than three unit cells thick.

Figure 3 shows representative XRD spectra of the YBCO/PBCO multilayer, where the designed thicknesses of the YBCO and the PBCO layers of the multilayer were four cells and three cells thick, respectively. The combined total number of YBCO and PBCO layers was 5, and the multilayer was deposited on a PBCO buffer layer that was 15 cells thick. The satellite peaks (indicated by arrows in the figure) on either side of the main (00l) peak indicate that periodicity was achieved in this film. The modulation wavelength D, which is the sum of the individual YBCO and PBCO layer thicknesses, was calculated from the separation of these satellite peaks. The calculated D from the XRD spectra agreed well with the designed thickness of the multilayer. Thus, from XRD measurements of the multilayers, we determined the layer thickness of the multilayers precisely.

B. Magnetization properties

Figure 4 shows how the magnetization of a typical YBCO/PBCO multilayer depends on the applied magnetic field, which was applied perpendicular to the film. After a zero-field cooling process, the magnetization decreased rapidly as the applied field increased because of the large shape effect seen in thin films. In a magnetic field of several 10 Oe, magnetization reached its minimum value and then traced a hysteresis loop. In a perfectly diamagnetic region, we can assume that a sample is a uniformly magnetized ellipsoid and that the magnetization M in an applied magnetic field H_0 can be given as

$$M = -\frac{1}{4\pi}\frac{2R}{\pi d}H_0 , \qquad (1)$$

where R and d are the radius and the thickness of the film, respectively. The magnetization is enhanced by the factor R/d, which is about 10^4 in a typical thin film sample. The rapid decrease in magnetization after the zero-field cooling process (observed in Fig. 4) is due to this demagnetization effect. With increasing magnetic field, the perfect diamagnetism disappears in a relatively low

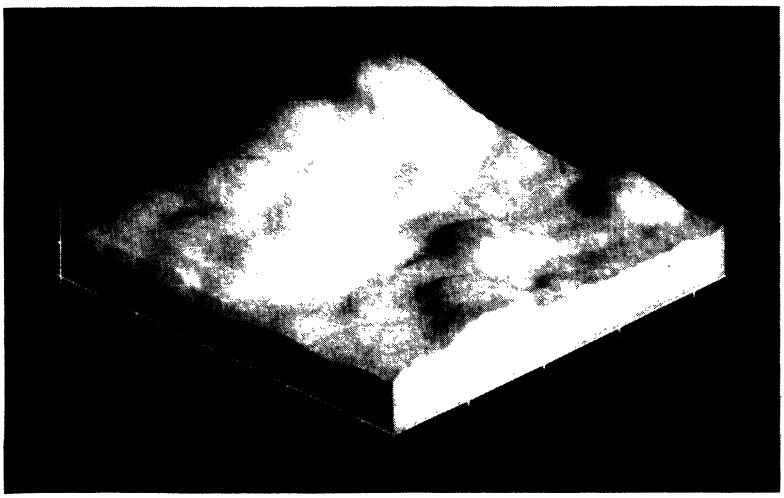

FIG. 2. AFM image of a typical YBCO/PBCO multilayered film, where the total thickness of the film was about 20 nm.

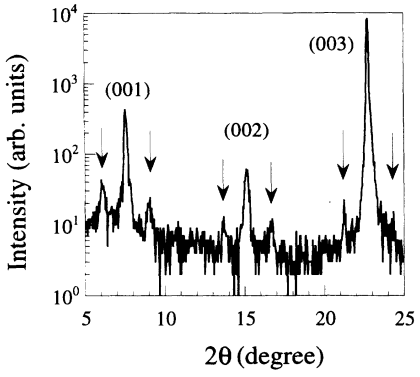

FIG. 3. X-ray diffraction spectra of a typical YBCO/PBCO multilayered film. Arrows indicate satellite peaks due to modulation.

magnetic field because of the large demagnetization effect, and the flux begins to penetrate inward from the edge of the film. In typical YBCO films, the flux meets at the center of the sample and the entire sample reaches critical state above 50 Oe, after which the magnetization traces the hysteresis loop (as clearly shown in Fig. 4).

The large hysteresis in the magnetization indicates that the films were uniform and had a high critical-current density. In previous work,[11] we observed both a large hysteresis in the magnetization and a uniform flux density distribution in epitaxial YBCO films. We also observed such a large magnetization in very thin films as well. Moreover, the small field dependence of the magnetization in a relatively low applied magnetic field suggested that there is no weak link and that a multilayer film with three-cell-thick YBCO layers has continuous superconductive layers. As described in a previous section, however, in films thinner than three unit cells, we did not observe large magnetization but rather very small magnetization. Therefore, a continuous layer that was two unit cells thick was not achieved over a large surface area using the present MBE technique. This is consistent with the surface morphology observed by AFM, which showed 1- or 2-nm steplike structures (Fig. 2)

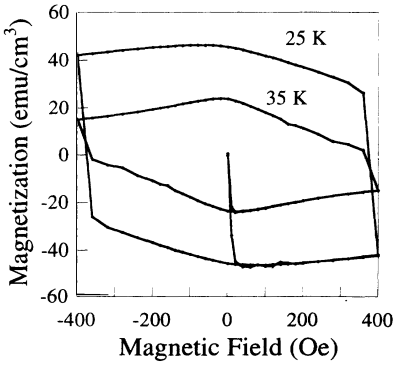

FIG. 4. Magnetic field dependence of the magnetization for a YBCO/PBCO multilayered film, where each YBCO and each PBCO layer is three cells thick. The magnetic field was applied perpendicular to the film surface.

For the measurements of J_c, we used a remanent magnetization measurement. First, a magnetic field was applied to the film sample that was well above T_c. The sample was then cooled in a constant magnetic field, after which the applied field was reduced by 200 Oe, which is enough for the entire sample to reach critical state. After the reduction of the applied field, the temperature was gradually increased to T_c and the positive remanent magnetization was measured. In the uniform epitaxial films with continuous superconductive layers, if we assume that the flux density distribution is uniform and if we use a simple, Bean critical state model, then a good approximation of J_c is

$$J_c = 30 M_{\rm rem}/R \ , \qquad (2)$$

where $M_{\rm rem}$ is the remanent magnetization and R is the sample radius (R was typically 0.3 cm in our samples). The films prepared by the present MBE technique showed a linear dependence of the magnetization on the radius of the disk-shaped samples.[11] Therefore, it is considered that the shielding current flows in the whole of a sample and we can take the radius of the sample as R. In the present work, the radius R was approximated by the radius of a circle that had the same area as the square sample.

The practical flux density distribution is, of course, not so simple, as seen in the magneto optical measurements of the flux density distribution.[12] In the present work, we discussed the temperature dependence of J_c and the simple, Bean critical state model is adequate in the case of uniformly thin films. The temperature dependence of J_c for the YBCO/PBCO multilayer was calculated using the Bean critical state model and is shown in Fig. 5.

C. Irreversibility lines

As shown in in Fig. 5, high J_c ($\sim 10^7 \mathrm{A/cm^2}$), which indicates good quality in a film, was seen for the low temperatures. For each level of applied magnetic field, as the

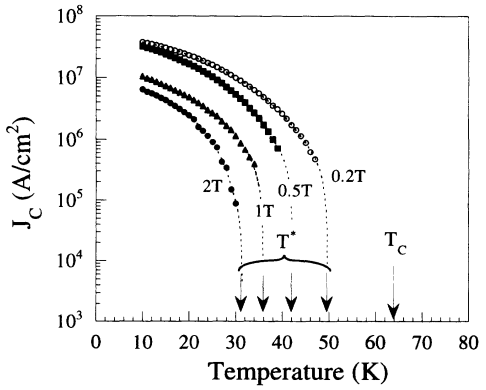

FIG. 5. Temperature dependence of J_c for YBCO/PBCO multilayered films determined from the remanent magnetization. The thickness of each YBCO and each PBCO is three cells. The dashed lines are an extrapolation using a polynominal expression.

temperature increased, J_c decreased monotonically and went to zero at T^*, just below T_c. Above T^*, the magnetization of the film was reversible. We defined the irreversibility temperature T^* as the temperature at which J_c became less than 1000 A/cm^2, which corresponds to the magnetic moment of 10^{-7} emu (the detection limits in the measurements of typical thin films). Usually, the precise measurements of the magnetic moment of 10^{-7} emu are difficult and we extrapolated the temperature dependence of magnetization using polynominal expressions and determined the irreversibility temperature, T^*.

Figure 6 shows the applied magnetic field vs T^*, in other words, the irreversibility lines for different YBCO/PBCO multilayered films. With increasing thickness of the PBCO layers, T^* decreased slightly for the same thickness of YBCO layers. It is well known that T_c of YBCO/PBCO multilayers that have very thin YBCO layers is lower than that of the bulk YBCO and decreases with increasing PBCO layer thickness when the thickness of the PBCO layers is several unit cells.[1] In the present work, we also observed that the T_c of the YBCO/PBCO multilayers decreases gradually with increasing PBCO layer thickness. This decrease in T_c is thought to cause the decrease in T^* (shown in Fig. 6). At the present stage, we consider that the slight change in the T_c in our samples was due to an extrinsic factor, such as an increase in disorder in the YBCO layers sandwiched between the thicker PBCO layers.

To clarify the intrinsic temperature dependence of the irreversibility line in YBCO/PBCO multilayers, we looked at the reduced temperature dependence of the irreversibility field. As clearly shown in Fig. 7, the irreversibility lines of all YBCO/PBCO multilayers coincide when the YBCO were three cells thick, even though the PBCO layers differed in thickness. In the high-temperature region, the irreversibility line $H(T^*)$ is well described by the TAFF model, which is a power-law function

$$H(T^*) \propto (1 - T^*/T_c)^{3/2} . \qquad (3)$$

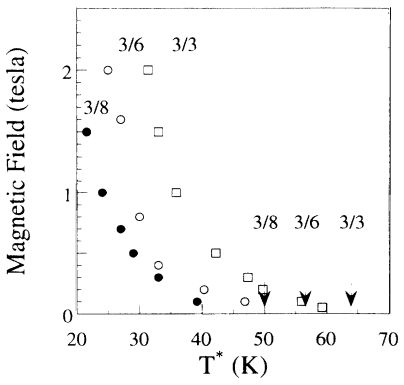

FIG. 6. Irreversibility line of YBCO/PBCO multilayered films. The ratio n/m represents the thickness of the YBCO layer (n) and that of the PBCO layer (m) in units of number of cells. T_c of the films is indicated by the arrows.

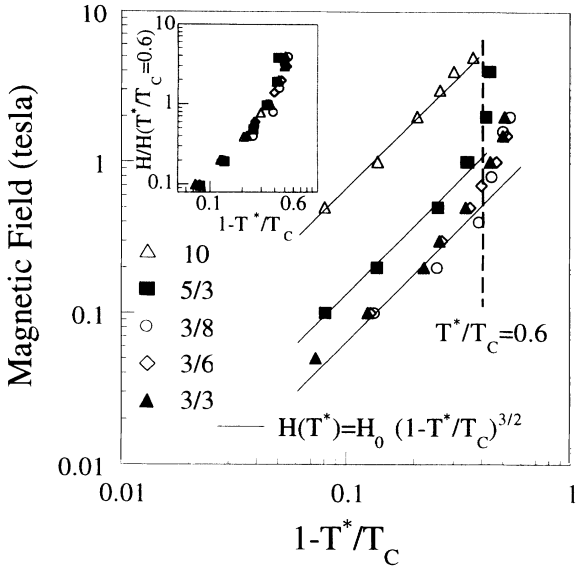

FIG. 7. Reduced temperature dependence of the irreversibility field in YBCO/PBCO multilayered films and in a ten-cell-thick single YBCO layer. The inset shows the temperature dependence of the normalized irreversibility fields.

At $T^*/T_c \sim 0.6$, however, the irreversibility line deviates from the TAFF power-law relationship, and increases more rapidly with decreasing temperature. Such a temperature dependence of the irreversibility line was common in all of the YBCO/PBCO multilayers, even though there were slight differences in T_c. For comparison, the irresistibility lines of the YBCO/PBCO multilayers and that of a single YBCO layer (the YBCO thicknesses of which were five and ten unit cells, respectively) are also shown in Fig. 7. The irresistibility line of the single YBCO layer that was ten unit cells thick was much higher than that of the multilayers with three-cell-thick YBCO layers, indicating that the irreversibility line strongly depends on the thickness of the YBCO layers. No change in the irreversibility lines for the multilayers with different PBCO layer thickness is clear evidence that YBCO layers separated by PBCO layers thicker than three unit cells were decoupled.

IV. DISCUSSION

A. Temperature dependence of irreversibility field

Even though the irreversibility lines of the thicker YBCO layers (i.e., the five-cell-thick YBCO/PBCO multilayer and the single, ten-cell-thick YBCO layer) are much higher than that of the YBCO/PBCO multilayers with three-cell-thick YBCO layers, the TAFF power law still applies. For the ten-cell-thick YBCO layer, the deviation at T^*/T_c, almost 0.6, could not be observed because the maximum applied magnetic field possible for our instrumentation was 5.5 T. Therefore, if we consider that T_c and the irreversibility field $H(T^*/T_c = 0.6)$ are

suitable fitting parameters, then the irreversibility lines for all the films studied here obey a universal scaling law (the inset of Fig. 7). This universal scaling behavior for the irreversibility line has also been observed in other high T_c bulk materials.[10] In the present study, we have clearly shown that the irreversibility line of very thin YBCO layers exhibits the same universal scaling behavior as that of bulk YBCO even though YBCO is considered to have a three-dimensional nature when compared with a Bi system. It indicates that the observed temperature dependence of the irreversibility line is very intrinsic for high-T_c materials

In contrast to this, the irreversibility field $H(T^*/T_c = 0.6)$, one of the fitting parameters in the universal scaling behavior of the irreversibility line, drastically decreased in very thin YBCO films. The dependence of the irreversibility field on YBCO thickness is shown in Fig. 8. The irreversibility field of bulk YBCO at $T^*/T_c = 0.6$ is considered to be 200 T (Ref. 10) and that of Bi 2:2:1:2, 0.02 T.[13] The irreversibility field of the YBCO/PBCO multilayers was lower than that of bulk YBCO and higher than that of Bi 2:2:1:2, and increased with increasing thickness of the YBCO layer. From the standpoint of the TAFF model, the irreversibility line is related to the activation energy of the flux motion U, which in turn is proportional to $R_c^2 L_c$, where R_c and L_c are correlation lengths perpendicular and parallel to the magnetic field, respectively. In the case of the YBCO/PBCO multilayers, L_c coincides with the YBCO thickness d_{YBCO} when R_c is constant.[7] The effect of the magnetic field on U was reported as $U \propto 1/\sqrt{H}$ for high-T_c materials that are more anisotropic, such as Bi systems,[14] and $U \propto 1/H$ for YBCO materials.[15] The irreversibility line is defined as the temperature and magnetic field when U reaches a certain value that is comparable to $k_B T$, where k_B is the Boltzmann constant. Therefore, for strong anisotropic systems, we predicted that

$$d_{\mathrm{YBCO}} \propto \sqrt{H(T^*/T_c = 0.6)} \ . \qquad (4)$$

As seen in Fig. 8, this relationship is consistent with our results for the YBCO/PBCO multilayers. Consequently, we conclude that the irreversibility field is correlated with the thickness of the YBCO layers, i.e., the anisotropy of the materials, and the irreversibility lines of YBCO/PBCO multilayers are analogous to that of the other high-T_c materials. For example, we project that the irreversibility field of YBCO/PBCO multilayers will decrease with decreasing thickness of the YBCO layers and will coincide with the irreversibility field of a Bi 2:2:1:2 system, indicating that Bi 2:2:1:2 is analogous to a YBCO/PBCO multilayer with very thin YBCO layers (0.7–0.8 nm). This thickness corresponds to correlation length of vortex parallel to the magnetic field and is shorter than the distance between CuO_2 planes of Bi 2:2:1:2, suggesting the strong two dimensionality of Bi systems. However, a continuous layer of such a very thin YBCO layer cannot be fabricated even when a sophisticated MBE technique (such as that used in this study) is used.

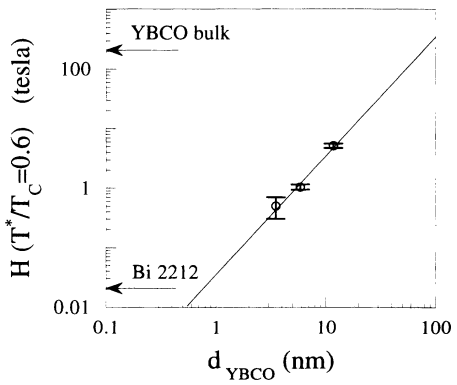

FIG. 8. Dependence of the irreversibility field at $T^*/T_c = 0.6$ on YBCO thickness. The irreversibility fields of bulk YBCO (Ref. 10) and Bi 2:2:1:2 (Ref. 13) are also shown. The solid line represents the relation, $d_{\mathrm{YBCO}} \propto \sqrt{H(T^*/T_c = 0.6)}$.

As observed in other high-T_c materials,[10] the deviation from the TAFF power-law relationship below $T^*/T_c = 0.6$ was also observed here in the YBCO/PBCO multilayers. The temperature dependence of the irreversibility field at low temperature was much stronger than that predicted from the TAFF model. Almasan *et al.*[10] claimed that the field strength at which the deviation from the TAFF power-law relationship occurs correlates with the penetration depth, and that the observed stronger temperature dependence of the irreversibility field is due to the collective effects of a vortex. In the case of the YBCO/PBCO multilayers, the deviation from the TAFF power-law relationship occurred at a much lower field strength than that of bulk YBCO and depended on the thickness of the YBCO layers. So it is not possible in this case that the origin of the deviation from the TAFF power-law relationship correlates with the penetration depth, nor is it due to the collective effects of a vortex.

B. Electric field E vs current density J characteristics

Recently, a vortex glass model for high-T_c materials has attracted special interest. From the standpoint of this model, the irreversibility line is considered to be the melting transition line of the vortex lattice or the vortex glass. The vortex glass model predicts that the power of the temperature dependence of the irreversibility field $H(T^*)$ is larger than the 3/2 predicted from the TAFF model. To discuss the vortex glass transition, measurements of the electric field E vs current density J characteristics are needed. If we neglect the geometric factor for our square-shaped samples, we can estimate the E-J characteristics of thin films in a very low electric field region using a relaxation measurement of magnetization.[16] Figure 9 shows the relationship between E and J for the ten-cell-thick single YBCO layer. In such a low electric field region, the E-J characteristics seemed to follow the vortex glass model rather than the TAFF model (linear dependence of E on J). To clarify the vortex

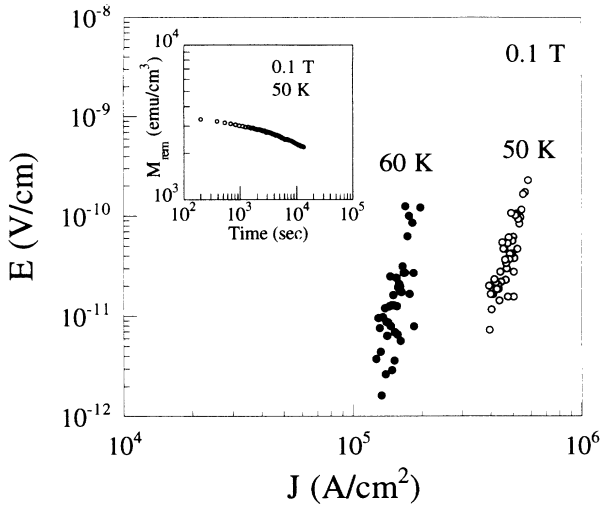

FIG. 9. E-J characteristics of the ten-cell-thick YBCO determined from the relaxation of remanent magnetization. The inset shows the time dependence of the remanent magnetization.

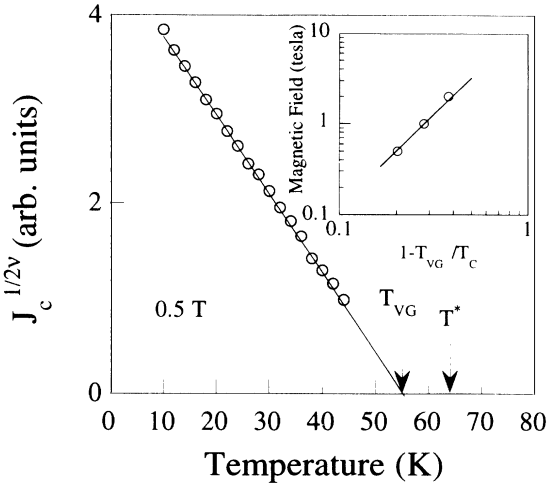

FIG. 10. The scaled temperature dependence of J_c for the ten-cell-thick single YBCO layer. The inset shows the scale temperature T_{VG} vs magnetic field. The solid line represents the relation, $H \propto (1 - T_{VG}/T_c)^2$.

states, the E-J characteristics at higher temperatures are needed, forcing us to measure the relaxation of magnetization near T_c. Using conventional dc magnetization measurements, however, the relaxation measurements at high temperatures are very difficult because of both the rapid decrease in magnetization and the small remanent magnetization.

The vortex glass behavior observed in the E-J characteristics at low temperature contrasts with the temperature dependence of the irreversibility field $H(T^*)$ at high temperatures that is consistent with the TAFF model. It is reasonable to consider that there are two regions of the vortex state in the films: One is the low-temperature region described by the vortex glass model and the other is the high-temperature region described by the TAFF model. To distinguish the vortex states of the YBCO/PBCO multilayers, we need to discuss in detail the temperature dependence of the remanent magnetization, i.e., J_c. From the vortex glass model, we can predict the power-law scaling of the physical properties in the vortex glass critical regime using the vortex glass transition temperature, T_{VG}. In the case of materials with strong enough random pinning, such as YBCO thin films, one expects that the physical properties are proportional to $(T-T_{VG})^{2\nu}$, where ν is the order of unit.[17] In the films with YBCO layers several cells thick, we found a power-law relationship for the temperature dependence of J_c using a temperature below T^*. Figure 10 shows this dependence for the ten-cell-thick single YBCO layer. The J_c of the films is well described by the expression

$$J_c \propto (T - T_{VG})^{2\nu} , \qquad (5)$$

where T_{VG} and ν are the fitting parameters. In the ten-cell-thick single YBCO layer, T_{VG} was lower than T^*, and ν was about 1. It is possible that a scaling behavior of J_c determined from the magnetization measurements with very low voltage criteria can be observed and that the above-mentioned scaling temperature, T_{VG}, be considered as the vortex glass transition temperature.

To confirm our estimation of the vortex glass transition, the scaling plot of the E-J characteristics using T_{VG} is shown in Fig. 11. We clearly see that the E-J curves at several temperatures are scaled using T_{VG} and are consistent with the vortex glass model. Consequently, we can consider that the T_{VG} is the vortex glass transition temperature. The values of J_c determined from usual dc magnetization measurements correspond to J at a certain low electric field, $J(E)$. Electric field dependence of J observed in the E-J characteristics shown in Fig. 9 was

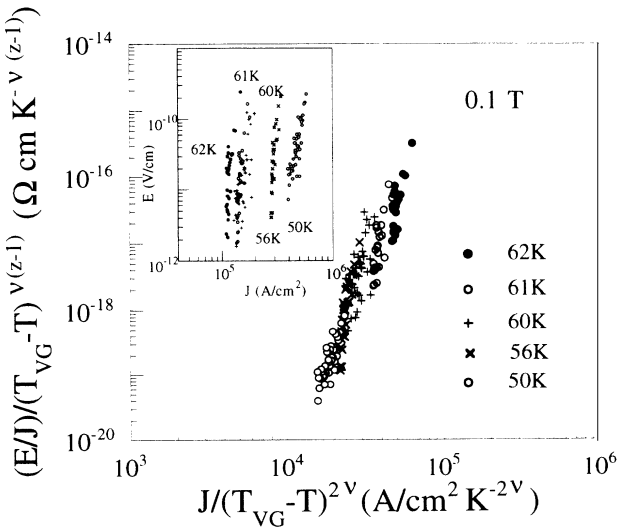

FIG. 11. Scaled and unscaled (inset) E-J plot for the ten-cell-thick single YBCO layer at several temperatures using the values $T_{VG} = 63.995$ K, $\nu = 0.61$, and $z = 4.8$ (Ref. 9).

very small, and the observed scaling properties of the J_c shown in Fig. 10 was due to the scaling properties of the E-J curves. Moreover, the wide critical region, at which J_c showed the power-law scaling, observed in the YBCO layer that was several cells thick is considered to be due to the strong anisotropy and low activation energy of vortex motion in very thin YBCO layers. For YBCO films thicker than ten unit cells, we could not observe a power-law scaling in such a wide temperature region and could not determined the vortex glass transition temperature from the temperature dependence of J_c.

C. Irreversibility line and vortex glass transition

The most important aspect of our work here is the observation of the vortex glass transition T_{VG} below the irreversibility temperature T^*. This indicates the existence of two vortex states, such as a liquid state and a solid (glass) state, in a conventionally determined nonzero J_c region. As shown in Fig. 12, for the ten-cell-thick single YBCO layer, the irreversibility line, i.e., $J_c = 0$ line, is always higher than the observed vortex glass transition line.

We determined the vortex glass transition line in the YBCO/PBCO multilayers, with the result shown in Fig. 13. The vortex glass transition line for the YBCO/PBCO multilayers with very thin YBCO layers (three cells thick) shows a stronger temperature dependence than that for the ten-cell-thick single YBCO layer. In the case of the YBCO/PBCO multilayer, it is most remarkable that the vortex glass transition line reached the irreversibility line at about $T/T_c = 0.6$–0.7, and that it coincided with the temperature when the irreversibility line changed its temperature dependence and deviated from the TAFF power-law relationship. Such crossover behavior can be explained as follows by the existence of the two vortex states.

In the high-temperature region, the vortex is in the liquid phase. However, if the so-called magnetic viscosity is relatively large, a small but nonzero J_c will be observed using some voltage criteria. The activation energy of

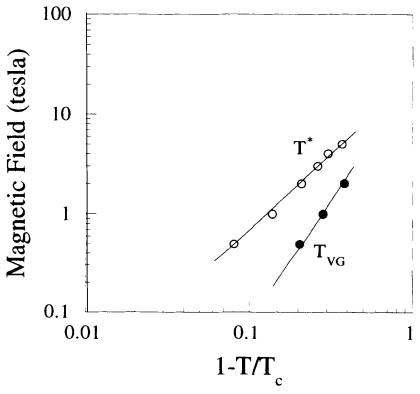

FIG. 12. Irreversibility line and vortex glass transition line for the ten-cell-thick single YBCO layer.

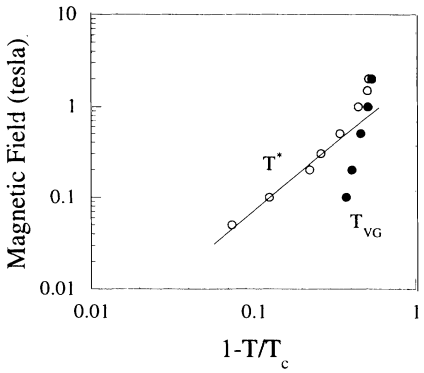

FIG. 13. Irreversibility lines and vortex glass transition line for the YBCO/PBCO (3/3) multilayered films.

the vortex motion U in a vortex liquid phase determines the irreversibility line, which shows the thermal activation behavior. The vortex glass transition temperature is below the irreversibility temperature. By decreasing the temperature and increasing the magnetic field, the vortex glass transition reaches the irreversibility line because the temperature dependence of the vortex glass transition is greater than that of the irreversibility line. After that point, the vortex state changes to the vortex glass state, and the dissipation mechanism of the flux motion completely changes. In the case of YBCO/PBCO multilayers, the crossover occurs at about $T/T_c = 0.6$. The irreversibility line below this crossover temperature is considered to be due to the vortex glass transition, i.e., the melting transition of vortex glass in the case of thin films. Therefore, it is naturally understood that the temperature dependence of the irreversibility line changes from the TAFF power-law dependence to the stronger dependence predicted from the vortex glass transition at the crossover temperature. This change of the temperature dependence in the irreversibility lines at about $T/T_c = 0.6$ was also observed in other high-T_c materials, and the crossover behavior at a certain reduced temperature observed in the YBCO/PBCO multilayers is considered an intrinsic property of high-T_c materials. For further study of the irreversibility line of high-T_c superconductors, of course, careful transport measurements of YBCO/PBCO multilayers are needed. In the present work, however, systematic magnetization measurements clarified that the vortex states in the YBCO/PBCO multilayers and the properties of the YBCO/PBCO multilayers are analogous to high-T_c materials that are more anisotropic, such as Bi systems.

V. CONCLUSION

In the present work, we performed systematic measurements of the magnetization in YBCO/PBCO multilayers and carefully determined the irreversibility line as the temperature and the applied magnetic field when the remanent magnetization goes to zero. Prior to measuring the superconductive properties of the multilayers, charac-

terization of the surface morphology of the films, which is very important for fabrication of layered structures, was carried out. We concluded that continuous YBCO layers thicker than three unit cells could be prepared using the present MBE technique. The result that for the YBCO/PBCO multilayers where the YBCO layers were three cells thick the irreversibility lines are identical even though the PBCO layers varied from three to eight cells thick indicates that the coupling between the YBCO layers via the PBCO layers disappears when the PBCO layer is thicker than three unit cells. The irreversibility field $H(T^*)$ increased rapidly with increasing the thickness of the YBCO layers and is considered to correlate with the anisotropy of the materials. The irreversibility field is high in YBCO, low in Bi systems, and intermediate in YBCO/PBCO multilayers. The thickness dependence of the irreversibility field of the YBCO/PBCO multilayers was consistent with the TAFF model. The irreversibility fields $H(T^*)$ of the YBCO/PBCO multilayers and the single YBCO films had a universal temperature dependence as observed in other high-T_c materials. Near T_c, the temperature dependence of the irreversibility lines of the films exhibited power-law behavior predicted from the TAFF model. Deviation from this behavior, however, was observed below $T^*/T_c = 0.6$. From the relaxation measurements of the magnetization, E-J characteristics at low temperature were consistent with the vortex glass model but not with the TAFF model. From careful measurement of the temperature dependence of J_c in the films, another transition line was observed below the irreversibility line. The E-J characteristics were scaled using another transition temperature and indicated the existence of a vortex glass transition below the irreversibility line. From these experimental results, we concluded that two vortex states exist below the irreversibility line and that the change in the temperature dependence of the irreversibility line is due to the crossover from the TAFF behavior in a vortex liquid state to the vortex glass behavior. We believe that further investigation into YBCO/PBCO multilayers will clarify the nature of the vortex state in high-T_c materials, which is very important for the application of these materials.

ACKNOWLEDGMENTS

The authors express their thanks to K. Kajimura for his encouragement throughout this research and to F. Hirayama for his help with the AFM measurements.

[1] J.-M. Triscone, Ø. Fischer, O. Brunner, L. Antognazza, A. D. Kent, and M. G. Karkut, Phys. Rev. Lett. **64**, 804 (1990).
[2] C. L. Jia, B. Kabius, H. Soltner, U. Poppe, K. Urban, J. Schubert, and Ch. Buchal, Physica C **167**, 463 (1990).
[3] Q. Li, X. X. Xi, X. D. Wu, A. Inam, S. Vadlamannati, W. L. McLean, T. Venkatesan, R. Ramesh, D. M. Hwang, J. A. Martinez, and L. Nazar, Phys. Rev. Lett. **64**, 3086 (1990).
[4] D. H. Lowndes, D. P. Norton, and J. D. Budai, Phys. Rev. Lett. **65**, 1160 (1990).
[5] T. Terashima, K. Shimura, Y. Bando, Y. Matsuda, A. Fujiyama, and S. Komiyama, Phys. Rev. Lett. **67**, 1362 (1991).
[6] H. Obara, S. Kosaka, M. Umeda, and Y. Kimura, Appl. Phys. Lett. **58**, 298 (1991).
[7] O. Brunner, L. Antognazza, J.-M. Triscone, L. Miéville, and Ø. Fischer, Phys. Rev. Lett. **67**, 1354 (1991).
[8] Y. Matsuda, S. Komiyama, T. Terashima, K. Shimura, and Y. Bando, Phys. Rev. Lett. **69**, 3228 (1992).
[9] C. Dekker, P. J. M. Wöltgens, R. H. Koch, B. W. Hussey, and A. Gupta, Phys. Rev. Lett. **69**, 2717 (1992).
[10] C. C. Almasan, M. C. de Andrade, Y. Dalichaouch, J. J. Newmeier, C. L. Seaman, M. B. Maple, R. P. Guertin, M. V. Kuric, and J. C. Garland, Phys. Rev. Lett. **69**, 3812 (1992).
[11] H. Obara, S. Kosaka, Y. Yokoyama, M. Umeda, and Y. Kimura, Phys. Rev. B **44**, 4532 (1991).
[12] Y. Yokoyama, Y. Suzuki, Y. Hasumi, H. Obara, T. Yosimi, Y. Kita, S. Kosaka, and S. Yoshida, Jpn. J. Appl. Phys. **30**, L1864 (1991).
[13] K. Kadowaki and T. Mochiku, Physica C **195**, 127 (1992).
[14] J. T. Kucera, T. P. Orlando, G. Virshup, and J. N. Eckstein, Phys. Rev. B **46**, 11 004 (1992).
[15] T. T. M. Palstra, B. Batlogg, R. B. van Dover, L. F. Schneemeyer, and J. V. Waszczak, Appl. Phys. Lett. **54**, 763 (1989).
[16] E. Sandvold and C. Rossel, Physica C **190**, 309 (1992).
[17] For a good review, see D. A. Huse, M. P. A. Fisher, and D. S. Fisher, Nature **358**, 553 (1992).

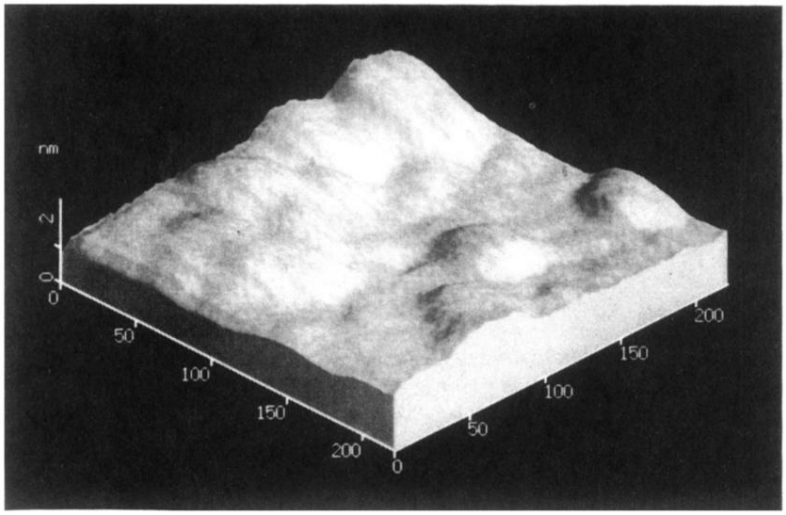

FIG. 2. AFM image of a typical YBCO/PBCO multilayered film, where the total thickness of the film was about 20 nm.